

# Local quantum criticality in confined fermions on optical lattices

M. Rigol and A. Muramatsu  
*Institut für Theoretische Physik III, Universität Stuttgart,  
Pfaffenwaldring 57, D-70550 Stuttgart, Germany.*

G.G. Batrouni  
*Institut Non-Linéaire de Nice, Université de Nice-Sophia Antipolis,  
1361 route des Lucioles, 06560 Valbonne, France*

R.T. Scalettar  
*Physics Department, University of California, Davis, CA 95616*

Using quantum Monte Carlo simulations, we show that the one-dimensional fermionic Hubbard model in a harmonic potential displays quantum critical behavior at the boundaries of a Mott-insulating region. A local compressibility defined to characterize the Mott-insulating phase has a non-trivial critical exponent. Both the local compressibility and the variance of the local density show universality with respect to the confining potential. We determine a generic phase diagram, that allows the prediction of the phases to be observed in experiments with ultracold fermionic atoms trapped on optical lattices.

PACS numbers: 03.75.Ss, 05.30.Fk, 71.30.+h

The Mott metal-insulator transition (MMIT), a paradigm of strong correlations, was recently realized in ultracold atoms confined on an optical lattice [1]. Due to the fact that the atoms interact only via a contact potential, this system constitutes the most direct experimental realization of the Hubbard model which is the prototype generally used to study the MMIT. Whereas optical lattices contain bosonic atoms, recent progress in cooling techniques allow fermionic systems to go well below the degeneracy temperature [2, 3], such that even superfluidity appears within reach [4]. It is therefore, to be expected that soon a fermionic MMIT will be realized on an optical lattice, offering the possibility to confront in a controlled way our knowledge of the MMIT in solid-state systems, without extrinsic effects always present there. This possibility is especially important since the MMIT is not only a long standing problem in condensed matter physics, but has also received renewed attention in recent years due to its different manifestations in a number of transition metal oxides, the most prominent being high temperature superconductors [5].

Motivated by the possibility of such crossfertilization, we performed QMC simulations for the ground-state of a one-dimensional Hubbard model with a harmonic potential, as in experiments with ultracold atoms, confining spin 1/2 fermions. The one-dimensional case was chosen since in one dimension, the quantum critical properties for the unconfined system are well characterized by the *Bethe Ansatz* solution where, in particular, the global compressibility  $\kappa \sim \partial n / \partial \mu$  diverges as  $\delta^{-1}$ , where  $\delta = 1 - n$ , and  $n$  is the expectation value of the density [6]. However, as shown theoretically [7] and numerically [8], in the presence of a confining potential the Mott-insulating phase is restricted to a domain that coexists with a compressible phase. This is in contrast to the global character typical of solid state systems. We show

in this Letter, that a properly defined local compressibility displays critical behavior on approaching the edges of the Mott-insulating phase, revealing a new critical exponent. Furthermore, it is shown that both the variance of the local density,  $\Delta_i \equiv \langle n_i^2 \rangle - \langle n_i \rangle^2$ , and the local compressibility as functions of the local density  $n_i$ , are independent of the confining potential for  $n_i \rightarrow 1$ . The exponents are also universal with respect to the strength of the interaction.

The Hamiltonian studied is as follows:

$$H = -t \sum_{i,\sigma} \left( c_{i\sigma}^\dagger c_{i+1\sigma} + h.c. \right) + U \sum_i n_{i\uparrow} n_{i\downarrow} + \left( \frac{2}{N} \right)^\alpha V_\alpha \sum_{i\sigma} \left( i - \frac{N}{2} \right)^\alpha n_{i\sigma}, \quad (1)$$

where  $c_{i\sigma}^\dagger$  and  $c_{i\sigma}$  are creation and annihilation operators, respectively, for a fermion on site  $i$  with spin  $\sigma = \uparrow, \downarrow$ . The local density per spin is  $n_{i\sigma} = c_{i\sigma}^\dagger c_{i\sigma}$ . The contact interaction is repulsive ( $U > 0$ ) and the last term models the potential of the magneto-optic trap. The QMC simulations were performed using a projector algorithm [9, 10, 11, 12], which applies  $\exp(-\theta H)$  to a trial wavefunction (in our case the solution for  $U = 0$ ). A projector parameter  $\theta \simeq 20/t$  suffices to reach well converged values of the observables discussed here. A time slice of  $\Delta\tau = 0.05/t$  was used in general.

Figure 1 shows density profiles along a harmonic trap ( $\alpha = 2$ ) for different fillings such that the system goes from an entirely metallic phase to a phase with insulating regions due to full occupancy of the sites, coexisting with metallic regions. At this point, such an identification is only based on the occupation number, using our knowledge from unconfined periodic systems. Although it is natural to identify the regions with  $n = 1$  as insulating phases, the global compressibility used in unconfined

systems is not a useful order parameter to characterize the phases due to the coexistence of local compressible regions with incompressible ones. A first quantity that can be used instead is the variance of the site density  $\Delta_i$ , since on entering the Mott-insulating region a suppression of double occupancy should occur, leading to a decrease of the variance.

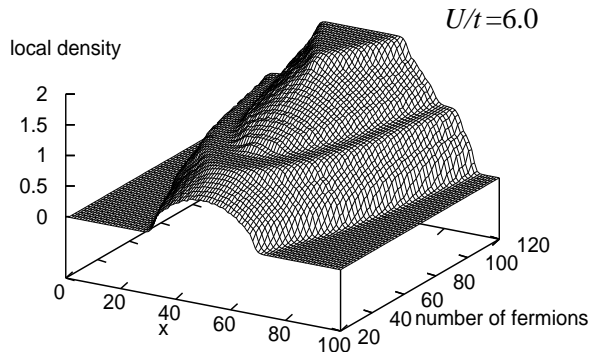


FIG. 1: Density profiles along the trap for different fillings. Flat terraces are the Mott insulating regions.

Figure 2 (a) shows three characteristic density profiles. In all of them,  $U/t = 6$  but depending on the filling ( $N_f$ ) and strength of the potential  $V_2$ , we obtain (i) an approximately parabolic density profile, indicating that the whole system is in a metallic phase. (ii) Increasing the number of particles, a Mott-plateau develops in the center of the system, and finally, (iii) with still a higher filling, a new metallic phase develops in the center of the plateau. The potential  $V_2$  was varied in order to obtain well developed phases. The corresponding profiles for the variance  $\Delta$  are shown in Fig.2(b). In general, a suppression of  $\Delta$  is present in the regions where the density profile shows a plateau. However, although in the region with  $n_i = 1$  the variance is lower than in the regions surrounding it, it does not vanish. Therefore, while the decrease of  $\Delta$  is a signature for the Mott-insulating phase, still a clearer distinction is needed. For this purpose we introduce a *local* compressibility defined as follows:

$$\kappa_i^l = \sum_{|j| \leq l(U)} \chi_{i,i+j}, \quad (2)$$

where  $\chi_{i,j}$  is the density-density correlation function. We take the length scale  $l(U) \simeq b\xi(U)$ , where  $\xi(U)$  is the correlation length given by  $\chi_{i,j}$  in the *unconfined* system at half filling for the given value of  $U$ . The value of  $b$  is such that  $\kappa^l$  becomes insensitive to the value chosen. In general we have  $b \sim 5 - 10$ , with  $\xi(U) \sim a$  ( $a$  is the lattice constant) for the values of  $U$  used here. The local compressibility thus gives the response to a constant shift of the potential over a finite range but over distances larger than  $\xi(U)$  in the periodic, unconfined system. If a region is in a Mott-insulating phase, and hence incompressible, no density response over distances larger than  $\xi$  is expected, leading to  $\kappa_i^l = 0$ . Figure 2(c) shows the

profile along the trap of  $\kappa_i^l$ , where the compressibility becomes zero in the outlying regions, where no particles are present and also where a Mott plateau is present. Therefore, the local compressibility defined here serves as a genuine local order parameter to describe the insulating regions that coexist, in general, with a surrounding metallic zone or even with metallic intrusions, beyond the intuitive pictures on the basis of the density profiles.

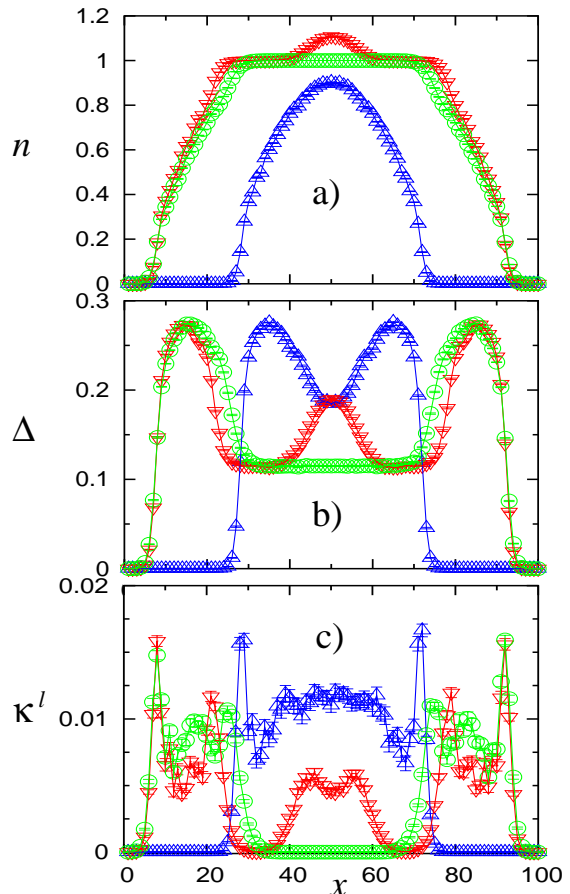


FIG. 2: (a) Density profiles for ( $\Delta$ )  $N_f = 30$ ,  $U = 6t$  and  $V_2 = 15t$ , ( $\circ$ )  $N_f = 70$ ,  $U = 6t$  and  $V_2 = 6.25t$ , and ( $\nabla$ )  $N_f = 74$ ,  $U = 6t$  and  $V_2 = 7t$ . (b) Variance of the local density (c) Local compressibility  $\kappa^l$  as defined in eq. (2).

Now that phases can be characterized quantitatively, we concentrate on the regions where the system goes from one phase to another. Criticality can arise, despite the microscopic spatial size, due to the extension in imaginary time that reaches a thermodynamic limit at  $T = 0$ , very much like the case of the single impurity Kondo problem [13], where long-range interactions in imaginary time appear for the local degree of freedom as a result of the interaction with the rest of the system. Recent experiments leading to a MMIT [1] consider a system with linear dimension  $\sim 65a$ , i.e. still in this microscopic range. An intriguing future question, for both theory and experiment, will be the role of spatial dimension in the critical behavior of systems in the thermodynamic limit.

Figure 3 shows the local compressibility *vs.*  $\delta$  for  $\delta \rightarrow 0$  in a double logarithmic plot. A power law  $\kappa^l \sim \delta^\varpi$  is obtained, with  $\varpi < 1$ , such that a divergence results in its derivative with respect to  $n$ , showing that critical fluctuations are present in this region. Since the QMC

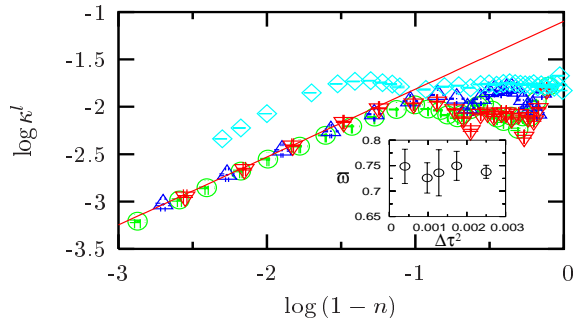


FIG. 3: The local compressibility  $\kappa^l$  *vs.*  $\delta = 1 - n$  at  $\delta \rightarrow 0$  for ( $\triangle$ )  $N_f = 70$ ,  $U = 8t$  and  $V_2 = 6.25t$ ; ( $\nabla$ )  $N_f = 70$ ,  $U = 6t$  and  $V_2 = 6.25t$ ; ( $\circ$ )  $N_f = 72$ ,  $U = 6t$  and a quartic potential with  $V_4 = 6.25t$ ; ( $\diamond$ ) unconfined periodic system with  $U = 6t$ . Inset: Dependence of the critical exponent  $\varpi$  on  $\Delta\tau^2$ .

simulation is affected by systematic errors due to discretization in imaginary time, it is important to consider the limit  $\Delta\tau \rightarrow 0$  in determining the critical exponent. The inset in Fig. 3 shows such an extrapolation leading to  $\varpi \simeq 0.68 - 0.78$ . At this point we should remark that the presence of the harmonic potential allows the determination of the density dependence of various quantities with unprecedented detail on feasible system sizes as opposed to unconfined periodic systems, where systems with  $10^3 - 10^4$  sites would be necessary to allow for similar variations in density. In addition to the power law behavior, Fig. 3 shows that for  $\delta \rightarrow 0$ , the local compressibility of systems with a harmonic potential but different strengths of the interaction or even with a quartic confining potential, collapse on the same curve. Hence, universal behavior as expected for critical phenomena is observed also in this case. This fact is particularly important with regard to experiments, since it implies that the observation of criticality should be possible for realistic confining potentials, and not only restricted to perfect harmonic ones, as usually used in theoretical calculations. However, Fig. 3 shows also that the unconfined case departs from all the others. Up to the largest systems we simulated (400 sites), we observe an increasing slope rather than the power law of the confined systems.

Having shown that the local compressibility displays universality on approaching a Mott-insulating region, we consider the variance  $\Delta$  as a function of the density  $n$  for various values of  $U$  and different confining potentials. Figure 4 shows  $\Delta$  *vs.*  $n$  for a variety of systems, where not only the number of particles and the size of the system are changed, but also different forms of the confining potential were used. Here we considered a harmonic potential, a quartic one, and a superposition of a harmonic, a cubic and a quartic one, such that even reflection symmetry

across the center of the system is broken. It appears at first glance that the data can only be distinguished by the strength of the interaction  $U$ , showing that the variance is rather insensitive to the form of the potential. The different insets, however, show that a close examination leads to the conclusion that only near  $n = 1$  and only in the situations where at  $n = 1$  a Mott-insulator exists, universality sets in. The inset for  $n$  around 0.6 and

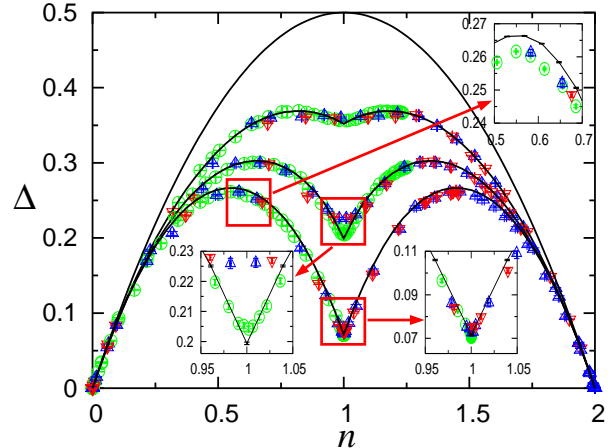


FIG. 4: a) Variance  $\Delta$  *vs.*  $n$  for ( $\circ$ ) harmonic potential  $V_2 = 6.25t$  with  $N = 100$ ; ( $\triangle$ ) quartic potential  $V_4 = 15.82t$  with  $N = 150$ ; ( $\nabla$ ) harmonic potential  $V_2 = 10t$  + cubic  $V_3 = 2.5t$  + quartic  $V_4 = 7.5t$  with  $N = 50$ ; and (full line) unconfined periodic potential with  $N = 102$  sites. The curves correspond from top to bottom to  $U/t = 0, 2, 4, 8$ . For a discussion of the insets, see text.

$U = 8t$ , shows that the unconfined system has different variance from the others albeit very close on a raw scale. This difference is well beyond the error bars. Also the inset around  $n = 1$  and for  $U = 4t$ , shows that systems that do not form a Mott insulating phase in spite of reaching a density  $n = 1$ , have a different variance from those having a Mott-insulator. The features above show that even a very local quantity like the variance cannot be accurately described using a local density approximation (Thomas-Fermi) [14], and can lead to even qualitatively wrong results, as for  $U = 4t$  and  $n = 1$ , where such an approximation would predict a Mott-insulator instead of a metal as in our simulations. Only the case where all systems have a Mott-insulating phase at  $n = 1$  ( $U = 8t$ ), shows universal behavior independent of the potential, a universality that encompasses also the unconfined systems. For the unconfined system, the behavior of the variance can be examined with Bethe-*Ansatz* [15] in the limit  $\delta \rightarrow 0$ . In this limit and to leading order in  $\delta$ , the ground state energy is given by [16]  $E_0(\delta)/N - E_0(\delta = 0)/N \propto \delta$ , such that the double occupancy, which can be obtained as the derivative of the ground-state energy with respect to  $U$ , will also converge as  $\delta$  towards its value at half-filling. Such behavior is also obtained in our case as shown by the inset at  $n = 1$  ( $U = 8t$ ) in Fig. 4. Detailed data for the variance close to  $n = 1$  will be presented elsewhere.

Finally we consider the phase diagram of the system. As shown in Fig. 2, unlike the exponents, phase boundaries seem to be rather sensitive to the choice of potential, number of particles and strength of the interaction. As in the unconfined case, we would expect to be able to relate systems with different number of particles and/or sizes by their density. Given the harmonic potential, a characteristic length (in units of the lattice constant) is given by  $N(4V_2/t)^{-1/2}$ , such that a characteristic density can be defined. Figure 5 shows that the characteristic density  $\tilde{\rho} = \rho\sqrt{4V_2/t}$  ( $\rho = N_f/N$ ) is a meaningful quantity to characterize the phase diagram. There, the phase dia-

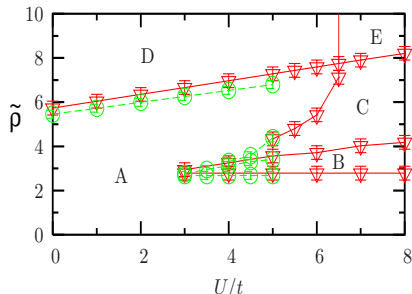


FIG. 5: Phase diagram for a system with  $N = 100$  ( $\nabla$ ) and  $N = 150$  ( $\circ$ ) sites. The phases are explained in the text.

grams for two systems with different sizes ( $N = 100$  and  $N = 150$ ) and different strength of the harmonic potential ( $V_2 = 15t$  and  $V_2 = 11.25t$  respectively) are depicted showing that such a scaling allows to compare systems with different sizes, different number of particles, and different strength of the potential. This makes it possible to relate the results of numerical simulations to much larger experimental systems. The different phases obtained are: A pure metal without insulating regions (A), a Mott-insulator at the center of the trap (B), a metallic intrusion at the center of a Mott-insulator (C), a “band insulator” (i.e. with  $n = 2$ ) at the center of the trap surrounded by a metal (D), and finally a “band insulator” surrounded by a metal, surrounded by a Mott-insulator with the outermost region being again a metal (E). Two features are remarkable here. The first one is that on varying the filling of the trap, a reentrant behavior is ob-

served for the phase A. The density profile shows a shoulder as can be seen in Fig. 1 before reaching the plateau with  $n = 2$  but, as shown by the inset of Fig. 4 for  $U = 4$  around  $n = 1$ , it is possible to go through a region with  $n = 1$  without reaching the value of the variance that corresponds to a Mott-insulator. The second intriguing feature is that the boundary between the regions A and B remains at the same value of the characteristic density for all values of  $U$  that could be simulated.

In summary, on the basis of QMC simulations of the Hubbard model with a harmonic potential, we found a number of new and unexpected features for the MMIT. (i) A local compressibility  $\kappa^l$  that appropriately characterizes Mott-insulating regions, shows critical behavior on entering those regions. Due to the microscopic nature of the phases, spatial correlations appear not to contribute to the critical behavior discussed here. This is a new form of MMIT, not observed so far in simple periodic systems, that might be realized in fermionic gases trapped on optical lattices. Therefore, our observation adds a new aspect to this long-standing problem in condensed matter physics. We expect that a similar local critical behavior will arise in higher dimensions as long as the spatial extent of the Mott domain remains finite. (ii) Universal behavior is found for  $\kappa^l$  for  $n \rightarrow 1$ , independent of the confining potential and/or strength of the interaction, excluding, however, the unconfined case. Also universal behavior is found for the variance  $\Delta$  when  $n \rightarrow 1$ . In this case, this behavior is shared by the unconfined model. (iii) Finally, a proper scaling form for a characteristic density is introduced that leads to a generic phase diagram, with interesting features, as described in the paragraph above.

We wish to thank HLR-Stuttgart (Project DynMet) for allocation of computer time. We gratefully acknowledge financial support from the LFSP Nanomaterialien, a PROCOPE grant (France-Germany), NSF-CNRS-12929, NFS-DMR-9985978, NSF-DMR-0312261, and NFS-INT-0124863. We are indebted to M. Arikawa, F. Göhmann, and A. Schadschneider for instructive discussions on Bethe-Ansatz, and to M. Feldbacher, B. O. Cult and F.F. Assaad for interesting discussions.

- 
- [1] M. Greiner *et al.*, Nature **415**, 39 (2002).  
[2] Z. Hadzibabic *et al.*, Phys. Rev. Lett. **88**, 160401 (2002).  
[3] G. Roati, F. Riboli, G. Modugno, and M. Inguscio, Phys. Rev. Lett. **89**, 150403 (2002).  
[4] K. O’Hara *et al.*, Science **298**, 2179 (2002).  
[5] M. Imada, A. Fujimori, and Y. Tokura, Rev. Mod. Phys. **70**, 1039 (1998).  
[6] T. Usuki, N. Kawakami, and A. Okiji, Phys. Lett. A **135**, 476 (1989).  
[7] D. Jaksch *et al.*, Phys. Rev. Lett. **81**, 3108 (1998).  
[8] G. Batrouni *et al.*, Phys. Rev. Lett. **89**, 117203 (2002).  
[9] G. Sugiyama and S. E. Koonin, Annals of Phys. **168**, 1 (1986).  
[10] S. Sorella, S. Baroni, R. Car, and M. Parinello, Europhys. Lett. **8**, 663 (1989).  
[11] E. Y. Loh and J. E. Gubernatis, in *Modern Problems of Condensed Matter Physics*, edited by W. Hanke and Y. Kopayev (North Holland, Amsterdam, 1992).  
[12] M. Imada, *Quantum Monte Carlo Methods in Condensed Matter Physics* (World Scientific, Singapore, 1993).  
[13] G. Yuval and P. Anderson, Phys. Rev. B **1**, 1522 (1970).  
[14] D. Butts and D. Rokhsar, Phys. Rev. A **55**, 4346 (1997).  
[15] E. H. Lieb and F. Y. Wu, Phys. Rev. Lett. **20**, 1445 (1968).  
[16] A. Schadschneider and J. Zittartz, Z. Phys. B **82**, 387 (1991).